BIOMOLECULES & THERAPEUTICS

Original Article
Biomol Ther 27(3), 290-301 (2019)

Involvement of a Novel Organic Cation Transporter in Paeonol Transport Across the Blood-Brain Barrier

Asmita Gyawali, Sokhoeurn Krol and Young-Sook Kang*

College of Pharmacy, Sookmyung Women's University, Seoul 04310, Republic of Korea

Abstract

Paeonol has neuroprotective function, which could be useful for improving central nervous system disorder. The purpose of this study was to characterize the functional mechanism involved in brain transport of paeonol through blood-brain barrier (BBB). Brain transport of paeonol was characterized by internal carotid artery perfusion (ICAP), carotid artery single injection technique (brain uptake index, BUI) and intravenous (IV) injection technique *in vivo*. The transport mechanism of paeonol was examined using conditionally immortalized rat brain capillary endothelial cell line (TR-BBB) as an *in vitro* model of BBB. Brain volume of distribution (V_D) of [^{3}H]paeonol in rat brain was about 6-fold higher than that of [^{14}C]sucrose, the vascular space marker of BBB. The uptake of [^{3}H]paeonol was concentration-dependent. Brain volume of distribution of paeonol and BUI as *in vivo* and inhibition of analog as *in vitro* studies presented significant reduction effect in the presence of unlabeled lipophilic compounds such as paeonol, imperatorin, diphenhydramine, pyrilamine, tramadol and ALC during the uptake of [^{3}H]paeonol. In addition, the uptake significantly decreased and increased at the acidic and alkaline pH in both extracellular and intracellular study, respectively. In the presence of metabolic inhibitor, the uptake reduced significantly but not affected by sodium free or membrane potential disruption. Similarly, paeonol uptake was not affected on OCTN2 or rPMAT siRNA transfection BBB cells. Interestingly. Paeonol is actively transported from the blood to brain across the BBB by a carrier mediated transporter system.

Key Words: Blood-brain barrier, Paeonol, Novel organic cationic transporter system, Brain transport, TR-BBB cells

INTRODUCTION

Paeonol (2'-hydroxy-4'-methoxyacetophenone) is a natural component and principle bioactive compound isolated from the root bark of Cortex Moutan (*Paeonia suffruticosa Andrew*) (Li *et al*., 2012). It possess various pharmacologic activities such as antioxidant, analgesic, anti-proliferative, anti-platelet aggregation, anti-neuroinflammatory, and anti-diabetic effects and counteraction for neurological disorders (Lin *et al*., 1999; Lau *et al*., 2007; Xu *et al*., 2007; Xie *et al*., 2008; Himaya *et al*., 2012; Liu *et al*., 2013; Zhao *et al*., 2014). It has been reported that paeonol derivatives are promising multifunctional agents for Alzheimer's disease (AD) and it can improve or relieve energy metabolism associated with brain development and ameliorate behavior in a rat model of AD (Palmer, 2011; Zhou *et al*., 2011). It is a protector of cerebrovascular damage and increases the level of acetylcholine (Palmer, 2011; Zhou *et al*., 2015). In addition, it has neuroprotective effect against brain diseases such as cerebral ischemic stroke, diabetic encephalopathy (DE), and AD (Xu *et al*., 2008; Zhong *et al*., 2009). Pharmacokinetics and metabolism of paeonol have been investigated through HPLC-DAD-MS method *in vivo* (Xie *et al*., 2008; Li *et al*., 2012). However, its transport mechanism across the blood-brain barrier (BBB) from blood to brain remain unknown. Distribution of drugs to the brain can be affected by various factors, including transport properties through BBB.

BBB is formed by tight junction of brain capillary endothelial cells and it plays an important role in the exchange of endogenous and exogenous substance in the blood (Misra *et al*., 2003; Abbott *et al*., 2010). To penetrate BBB via lipid-mediated free diffusion, molecular weight (MW) of substance must be less than 400 Dalton (Pardridge, 2005; Ohtsuki and Terasaki, 2007; Pardridge, 2012, 2015). Previous studies have reported that lipophilic organic cationic compounds can be transported across plasma membrane via several carrier mediated, organic cationic transport (OCT) family, organic cation/carnitine transporter (OCTN) family, and plasma membrane

Open Access **https://doi.org/10.4062/biomolther.2019.007**

Received Jan 17, 2019 **Revised** Feb 15, 2019 **Accepted** Feb 20, 2019
Published Online Apr 1, 2019

***Corresponding Author**
E-mail: yskang@sm.ac.kr
Tel: +82-2-710-9562, Fax: +82-2-710-9871

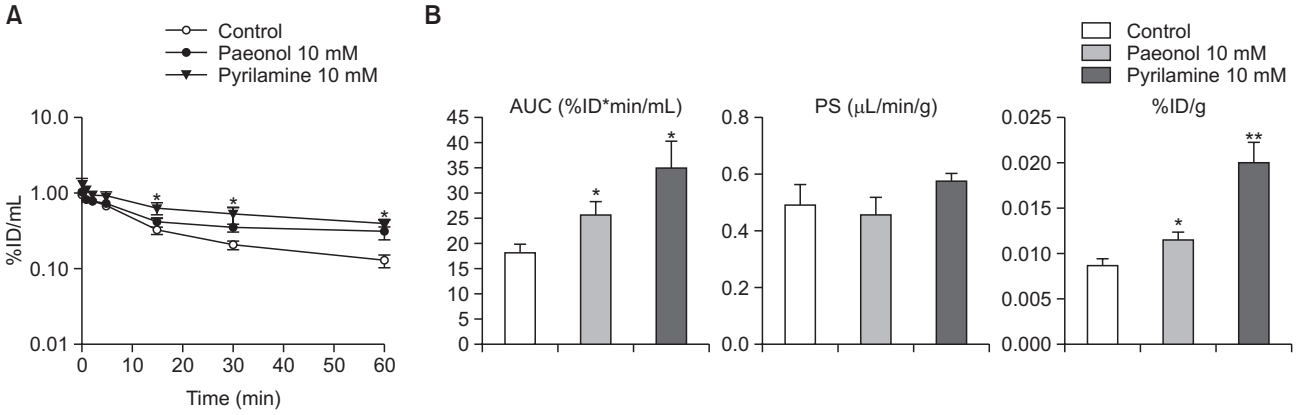

Fig. 1. Plasma clearance profile of [^{3}H]paeonol (○), paeonol 10 mM (●) and pyrilamine 10 mM (▼) for up to 60 min after single intravenous (IV) injection (A) and 60-min plasma AUC (%ID*min/mL), BBB PS product (μL/min/g) and brain distribution (%ID/g) in SD rats (B). Data are presented as mean ± SEM (n=3). *p<0.05, **p<0.01 significantly different from control.

monoamine transporter (PMAT) (Pardridge, 2012; Kubo *et al*., 2013b). Recently, it has been found that lipophilic compounds such as diphenhydramine, pyrilamine, oxycodone, tramadol, clonidine, amantadine, cocaine, memantine, nicotine, and apomorphine are transported from circulating blood to the brain via organic cation-sensitive transporter and carrier mediated transporter system (Bostrom *et al*., 2006; Okura *et al*., 2008; Andre *et al*., 2009; Sadiq *et al*., 2011; Kooijmans *et al*., 2012; Cisternino *et al*., 2013; Shimomura *et al*., 2013; Tega *et al*., 2013; Chapy *et al*., 2014; Kitamura *et al*., 2014; Okura *et al*., 2014a; Higuchi *et al*., 2015; Tega *et al*., 2015a). Paeonol has a small molecular weight (166.17 g/mol) and high lipophilicity (2.31, pH 7.4) with pKa value of 9.78 so it could be easily transported to the brain. However, the transport mechanism of paeonol is still unknown. Therefore, the objective of our study was to investigate the transport mechanism of paeonol to the brain through BBB using both *in vitro* (using conditionally immortalized rat brain capillary endothelial cell line (TR- BBB) as a model of BBB) and *in vivo* (using internal carotid artery perfusion) ICAP, carotid artery single injection technique (brain uptake index, BUI) and intravenous (IV) injection techniques.

MATERIALS AND METHODS

Radioisotopes and reagents

Radiolabeled compounds [^{3}H]paeonol (7.2 Ci/mmol), 3-0-Acetyl-L-carnitine [N methyl-^{3}H-] hydrochloride ([^{3}H]ALC, 60 Ci/mmol), and N-methy-4-phenylpyridinium [N-methyl-^{3}H-], ([^{3}H]MPP$^+$, 83.9 Ci/mmol), were purchased from American Radiolabeled Chemicals, Inc (St. Louis, MO, USA). Bovine serum albumin (BSA) and Bio-Rad DC protein assay kit were purchased from Bio-Rad Laboratories Co (Hercules, CA, USA). Unlabeled compounds such as paeonol, imperatorin, tramadol hydrochloride, pyrilamine maleate salt, quinidine, verapamil, tetraethyl ammonium (TEA), choline, estrone 3-sulfate sodium salt (E.S.), para-aminohippurate (PAH), dopamine, ALC (acetyl-L-carnitine), 1-methyl-4-phenylpyridinium (MPP$^+$), diphenhydramine, 6-mercuptopurine (6-MP), mannitol, and other compounds were purchased from Sigma Aldrich (St. Louis, MO, USA).

Animals

Male Sprague-Dawley rats (SD rats, 7 weeks, 230-350 g) were purchased from Koatech Inc (Pyeongtaek, Korea). These animals were housed at 25°C for 12 h dark and 12 h light cycle. All animal experiments were approved by the Committee of the Ethics of Animal Experimentation of Sookmyung Women's University (SMWU-IACUC-1405-009-03).

Pharmacokinetics and brain uptake by intravenous injection (IV) technique

Pharmacokinetics studies were performed using procedures described previously (Kang *et al*., 1995; Lee *et al*., 2014b). Male SD rats were intramuscularly anesthetized with ketamine/xylazine (100 mg/kg / 2 mg/kg) (Yuhan, Seoul, Korea). The left femoral vein was cannulated with a polyethylene-50 (PE-50) tubing (SP-45, Natsume, Tokyo, Japan) and injected with a 0.2 mL Ringer-Hepes buffer including serum albumin 1% at pH 7.4 and [^{3}H]paeonol (5 uCi/ 695 nM). Blood samples (0.3 mL) were collected at 0.25, 1, 2, 5, 15, 30, and 60 min after the injection. These animals were decapitated to remove the brain and other organs (heart, liver, lung, and kidney) at 60 min after IV injection. These organs were solubilized with Soluene 350 (PerkinElmer Inc., Waltham, MA, USA) before liquid scintillation counting at 60°C for 3 h. Each sample was mixed with 10 mL of Ultima gold (PerkinElmer Inc.) to analyze radioactivity using Tri-Carb Liquid Scintillation Counters (PerkinElmer).

Pharmacokinetic parameters were computed as described previously (Kang *et al*., 1995; Lee *et al*., 2014b). The radioactivity in the plasma (dpm/mL) was converted to percentage of injected dose (ID) per milliliter (mL) and the % ID/mL was fit to the following bi-exponential equation:

$$\%ID/mL = A_{1e}^{(-k_1 t)} + A_{2e}^{(-k_2 t)} \quad (1)$$

The intercepts A_1 and A_2 and slopes K_1 and K_2 were used to calculate the pharmacokinetic parameters such as area under the plasma concentration curve at 60 min (AUC), steady-state AUC (AUC_{ss}) steady state volume of distribution ($V_{d.ss}$) and systemic clearance (CL) (Lee *et al*., 2014b).

The permeability-surface area (PS) product of BBB was determined using the following equation:

Table 1. Pharmacokinetic parameters of [^{3}H]paeonol after single intravenous (IV) injection in SD rats

Parameter	[^{3}H]Paeonol	+ Paeonol 10 mM	+ Pyrilamine 10 mM
$T_{1/2}$ (min)	28.9 ± 2.5	84.9 ± 18.3*	43.3 ± 7.5
AUCss (%ID* min/mL)	23.2 ± 2.4	63.3 ± 9.8*	60.6 ± 12.1*
$V_{d,ss}$ (mL/kg)	161 ± 14	189 ± 27	111 ± 11
CL (mL/min/kg)	4.38 ± 0.47	1.67 ± 0.31*	1.77 ± 0.30*
MRT (min)	37.0 ± 2	118 ± 24*	65.4 ± 8.5*

Parameter computed from the plasma radioactivity profile in Fig. 1. V_D, BBB PS product, %ID/g and pharmacokinetic parameters were estimated after IV injection of [^{3}H]paeonol (694 nM) at 60 min in SD rat. Each value represents are mean ± SEM (n=3). *p<0.05 was significantly different from control. $T_{1/2}$, half-life; AUC, area under curve; CL, clearance; MRT, mean residence time; $V_{d,ss}$, plasma volume of distribution at steady state.

Table 2. Brain volume of distribution (V_D), BBB PS product, other organs distribution (%ID/g) of [^{3}H]paeonol after single intravenous (IV) injection in SD rats

	[^{3}H]Paeonol	+ Paeonol 10 mM	+ Pyrilamine 10 mM
V_D (μL/g)	82.0 ± 17.0	39.0 ± 9.0*	45.0 ± 1.0*
%ID/g			
Brain	0.0087 ± 0.0005	0.012 ± 0.001*	0.020 ± 0.002**
Heart	0.041 ± 0.007	0.086 ± 0.007	0.18 ± 0.05
Liver	0.078 ± 0.004	0.093 ± 0.004	0.15 ± 0.02
Lung	0.21 ± 0.1	0.17 ± 0.04	0.29 ± 0.07
Kidney	4.54 ± 0.26	7.03 ± 0.96*	7.26 ± 0.05**

Parameter computed from the plasma radioactivity profile in Fig. 1. V_D, BBB PS product, %ID/g and pharmacokinetic parameters were estimated after IV injection of [^{3}H]paeonol (694 nM) at 60 min in SD rat. Each value represents are mean ± SEM (n=3). *p<0.05, **p<0.01 was significantly different from control. $T_{1/2}$, half-life; AUC, area under curve; CL, clearance; MRT, mean residence time; $V_{d,ss}$, plasma volume of distribution at steady state.

$$PS = \frac{[V_D - V_0]Cp(T)}{\int_0^T Cp(T)dt} \quad (2)$$

Where, C_p (T) was the 60-min plasma concentration (% ID/mL), V_D was the brain volume of distribution or the terminal brain/plasma volume, and V_0 was the plasma volume for respective organ as described previously (Pardridge *et al*., 1994; Kang and Park, 2000). Terminal brain uptake expressed as %ID/g brain was calculated from the PS (μL/min/g) and the 60-min plasma of area under the curve (AUC) (% ID min/mL) using the following equation:

$$\%ID/g = PS \times AUC/1000 \quad (3)$$

Internal carotid artery perfusion technique

Internal carotid artery perfusion (ICAP) technique was carried out as described previously (Bickel *et al*., 1996; Lee and Kang, 2016). Briefly, the occipital artery, superior thyroid artery, and straight pterygopalatine artery were bound by electro cauterization. The external carotid artery was cannulated with polyethylene-10 tubing (SP-10, Natsume). The common carotid artery was ligated just before starting perfusion. Krebs-Henseleit buffer (KHB) containing 0.1% bovine serum albumin (BSA) was equilibrated with 95% O_2/5% CO_2 at 37ºC. The buffer contained 1 μCi/ 139 nM of [^{3}H]paeonol with or without inhibitory compounds. Perfusion was terminated by decapitation. The brain was removed quickly during 15 s of infusion with an infusion pump (Harvard Apparatus, South Natick, MA, USA; at 4 mL/min). The ipsilateral cortex of brain was weighed and solubilized in 3 mL Soluene 350. The [^{3}H] radioactivity was analyzed using the Tri-Carb Liquid Scintillation Counters.

Perfusion fluid

Briefly, the ionic composition of KHB perfusate was changed to remove Na+ and Cl- by iso-osmotic replacement (Chapy *et al*., 2014). Sodium and chloride were replaced by mannitol (256 mM mannitol) (Kooijmans *et al*., 2012; Cisternino *et al*., 2013). To change intracellular pH to alkalization condition, carbonate free HEPES buffer (mmol/L: (119 mM NaCl, 4.7 mM KCl, 25 $NaHCO_3$, 1.2 mM $MgSO_4$, 1.2 mM K_2HPO_4, 10 mM HEPES, 2.5 mM $CaCl_2$, 10 mM D-glucose and 10 g/dl BSA) was used.

Apparent brain distribution volume and initial brain transporter parameters

Data analysis for brain uptake ratio of [^{3}H]paeonol to perfusate was performed as described previously (Kang *et al*., 1995). Briefly, the apparent brain volume of distribution (V_D) of [^{3}H]paeonol was determined from the ratio activity of disintegrations per min per gram (dpm/g) of brain to disintegration per min per microliter (dpm/μL) of perfusate (Pardridge *et al*., 1994).

$$_D(\mu L) = \frac{[\text{brain (dpm)/brain (g)}]}{[\text{perfusate (dpm)/perfusate (}\mu L)]} \quad (4)$$

The permeability surface area (PS) product of the BBB was calculated using the following equation:

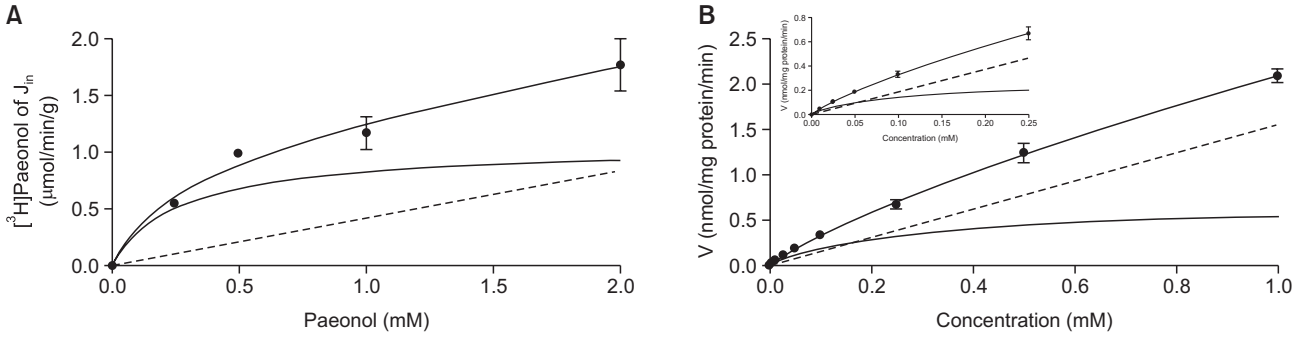

Fig. 2. Concentration dependence of [^{3}H]paeonol transport using ICAP *in vivo* (A) and TR-BBB cells *in vitro* (B). The uptake of [^{3}H]paeonol was measured by ICAP in the presence or absence of 0-2 mM unlabeled paeonol. It was measured in TR-BBB cells for 5 min with or without 0-1 mM unlabeled paeonol at pH 7.4. The solid curve, dotted line, and curve represent estimated total, non-saturation, and saturation uptakes, respectively. Data are presented as mean ± SEM (n=3-4).

Table 3. Inhibitory effect of various compounds on [^{3}H]paeonol brain transport in the rat brain following internal carotid artery perfusion in SD rats

Inhibitor	Concentration (mM)	Brain volume of distribution (V_D, μL/g)	Control (%)	(n)	Predicted Log D
Control		674 ± 30	100 ± 4	9	
Paeonol	1	292 ± 37**	43 ± 6**	3	2.31
	10	123 ± 21***	18 ± 3***	4	
Imperatorin	1	284 ± 39***	42 ± 6***	4	4.01
Tramadol	1	505 ± 29**	75 ± 4**	3	0.29
	10	463 ± 21**	69 ± 3**	3	
Diphenhydramine	10	353 ± 24***	52 ± 3***	3	3.43
Pyrilamine	10	422 ± 10***	63 ± 2***	3	0.76
MPP^+	10	477 ± 33**	71 ± 5**	3	–0.29
ALC	10	395 ± 32***	59 ± 5***	4	–3.43
Verapamil	1	472 ± 14**	70 ± 2**	3	2.46
Quinidine	1	488 ± 18**	72 ± 3**	3	0.98
TEA	10	642 ± 40	96 ± 6	3	–3.26
Choline	10	747 ± 67	111 ± 10	3	–4.14
6-MP	1	686 ± 9	101 ± 1	3	–3.09

ALC, acetyl-L-carnitine; MPP^+, 1-methyl-4-phenylpyridinium; TEA, tetraethylammonium; 6-MP, 6-Mercaptopurine.
Inhibition of [^{3}H]paeonol (13.9 nM) brain transport by other cold compounds (1-10 mM) was evaluated by internal carotid perfusion at rate of 4 mL/min for 15 s in SD rats, pH: 7.4. The data represent mean ± SEM (n=3-9). ***p*<0.01, ****p*<0.001 was significantly different from control.

$$PS\ (\mu L/min/g) = V_D\ (\mu L/g)/t\ (min) \quad (5)$$

Where t was the perfusion time (15 s).

For concentration-dependency experiment, the influx (J_{in}, μmol/min/g) of [^{3}H]paeonol was determined with equation:

$$J_{in} = PS \times C_{tot} \quad (6)$$

Where C_{tot} (mM) was the concentration of paeonol in the perfusate.

For saturable transport, [^{3}H]paeonol of brain influx (J_{in}) or cellular velocity (μmol/min/g) was described as a saturable Michaelis-Menten constant. Passive unsaturable compounds have been previously measured (Chapy *et al*., 2014).

$$J_{in} = \frac{V_{max}\ C_{tot}}{K_m + C_{tot}} + K_d\ C_{tot} \quad (7)$$

Where C_{tot} (mM) was total paeonol concentration in the perfusate or incubation buffer, V_{max} (μmol/min/g) was the maximal velocity of transport, and K_m (mM) of paeonol was the concentration at half-maximal carrier velocity. K_d (μL/min/g) was an unsaturable component transported by passive diffusion. Data were fitted using nonlinear regression analysis.

Brain uptake index method (BUI)

BUI method was performed to investigate the inhibition activity of various compound on [^{3}H]paeonol uptake by following the precious reports. (Suzuki *et al*., 2010; Tun and Kang, 2017). Ringer HEPES buffer containing [^{3}H]paeonol (2.5 μci) and [^{14}C]n-butanol (0.5 μci) with or without unlabeled compounds were injected in the right common carotid artery. Rat was decapitated 15 s after the injection and brain was isolated and dissolved in solunene-350. Radioactivity was measured using Tri-Carb Liquid scintillation counters. The percentage BUI was calculated using the following equation.

$$BUI\% = \frac{\frac{[3H]}{[14C]}(\text{dpm in th brain})}{\frac{[3H]}{[14C]}\text{dpm in the injected solution}} \times 100 \quad (8)$$

Cell culture

TR-BBB cells were cultured according to previous reports (Kang *et al*., 2005; Lee *et al*., 2012). Briefly, TR-BBB cells were seeded in rat tail collagen type 1-coated 24 well culture plates (Iwaki, Tokyo, Japan) at a density of 1×10^5 cells/well. Cells were maintained at 33°C under humidified atmosphere with 5% CO_2/95% air.

In vitro of [^{3}H]paeonol uptake studies in TR-BBB cells

The *in vitro* uptake study of [^{3}H]paeonol transport in TR-BBB cells was performed according to previous reports (Kang *et al*., 2002; Lee *et al*., 2014a; Tega *et al*., 2015b). Briefly, cells were washed three times with 1 mL extracellular fluid (ECF) buffer at pH of 7.4 and temperature of 37°C. Cells were then incubated with 200 μL ECF buffer containing 70 nM of [^{3}H] paeonol with or without inhibitory compounds at 37°C for designed time duration. Cells were washed three times with 1 mL cold ECF buffer to determinate the uptake. After overnight of incubation, cells of each plate were collected to examine the radioactivity using Tri-Carb Liquid Scintillation Counters (PerkinElmer). Protein concentration was determined using DC protein assay kit (Bio-Rad Laboratories Co) with bovine serum albumin as standard. The uptake of [^{3}H]paeonol was expressed as cell-to-medium (μL/mg protein) ratio. It was obtained by dividing the uptake amount by the concentration of substrate in the transport medium using the following equation:

$$\text{Cell/medium ratio (}\mu\text{L/mg protein)} = ([^3\text{H}]\text{dpm in the cell per mg protein})/([^3\text{H}]\text{dpm in the cell medium per }\mu\text{L}) \quad (9)$$

The uptake of [^{3}H]paeonol uptake at 0-1 mM was measured for 5 min as the initial uptake. To estimate kinetic parameters, the initial uptake of [^{3}H]paeonol at 0.01-0.25 mM for 5 min was fitted by Michaelis-Menten plot using the following equation :

$$V=V_{max}\times C/(K_m+C)+K_d\times C \quad (10)$$

Where V and C were the initial uptake rate of [^{3}H]paeonol at 5 min and the concentration of paeonol, respectively. V_{max} was the maximum uptake rate for saturable component (nmol/min/mg protein), K_m was the Michaelis-Menten constant (mM), and K_d was the first order constant for non-saturable component. V_{max}/K_m (μL/min/mg protein) value was calculated as the uptake clearance for saturable transport compound.

To analyze the competitive nature of inhibitors such as tramadol and pyrilamine for [^{3}H]paeonol uptake by TR-BBB cells, Lineweaver-Burk plots were obtained. Inhibitory constant (K_i) was calculated using the following equation:

$$V=V_{max}\times C/[K_m\times(1+I/K_i)+C] \quad (11)$$

Where I was inhibitor concentration (the concentration of each mutual inhibitory effect of a compound).

In order to determine the metabolic energy dependence of [^{3}H]paeonol uptake by TR-BBB cells, the uptake of [^{3}H]paeonol was measured under ATP-depleted condition by pre-incubation with 0.1% of sodium azide (NaN_3, metabolic energy inhibitor) for 20 min. In this experiment, 10 mM D-glucose in the transport buffer was replaced by 10 mM 3-*O*-methylgoucose to reduce metabolic energy. To examine sodium ion dependency of [^{3}H]paeonol uptake by TR-BBB cells, the uptake was measured under sodium ion-free condition by replacing with *N*-methylglucamine$^+$ (NMG^+). To examine the effect of membrane potential on [^{3}H]paeonol uptake, sodium ion was replaced with KCl or pretreated with 10 μM valinomycin (potassium ionophore) for 10 min in transport buffer containing 0.2% DMSO. In order to evaluate the effect of proton gradient on [^{3}H]paeonol uptake, cells were treated with 10 μM carbonyl cyanide-*p* trifluoromethoxyphenylhydrazone (FCCP, a protonophore, dissolved in the transport medium containing 0.2% ethanol) for 10 min (Okura *et al*., 2008; Tega *et al*., 2015b). The uptake of [^{3}H]paeonol was also measured at pH of 6.4, 7.4, and 8.4.

To examine the effect of intracellular pH (pH_i) on [^{3}H]paeonol uptake, NH_4Cl was used as described in previous study (Kitamura *et al*., 2014). NH_4Cl (30 mM) was simultaneously used to elevate alkalized pH_i (Sadiq *et al*., 2011). To measure the uptake of [^{3}H]paeonol at acidic pH_i, cells were pre-treated with 30 mM of NH_4Cl for 30 min.

Table 4. Brain uptake index (BUI) of [^{14}C]paeonol by SD rats

Inhibitor	Concentration (mM)	Control (%)	(n)
Control		100 ± 4	9
Paeonol	10	38 ± 2***	4
Imperatorin	1	53 ± 2***	3
Tramadol	10	50 ± 1***	3
Clonidine	10	59 ± 1***	3
Nicotine	10	58 ± 0.3**	3
Verapamil	3	47 ± 3***	3
Propranolol	10	55 ± 1**	3
Pyrilamine	10	55 ± 3***	3
Diphenhydramine	10	60 ± 3***	3
ALC	10	61 ± 3**	3
MPP^+	10	57 ± 1***	3
TEA	10	101 ± 1	3
PAH	10	102 ± 3	3
Choline	10	105 ± 3	3
Taurine	10	103 ± 2	3

ALC, acetyl-L-carnitine; MPP^+, 1-methyl-4-phenylpyridinium; TEA, tetraethylammonium; 6-MP, 6-mercaptopurine. The data represent mean ± SEM (n=3-9). **p<0.01, ***p<0.001 was significantly different from control.

Small interfering RNA transfection

In order to determine the functional role of transporter on brain uptake of [^{3}H]paeonol, transient knockdown of OCTN2 and rPMAT in TR-BBB cells was performed by transfection of small interfering RNA (siRNA) purchased from Dharmacon, GE (Landsmeer, the Netherlands). RNA interference analysis was performed as described in previous reports (Okura *et al*., 2011, 2014b; Lee and Kang, 2016). Briefly, TR-BBB cells were seeded at density of 1×10^5 cells/well on type I collagen-coated 24-well plates (Iwaki). After 60-70% confluence was achieved on the next day, cells were transfected with OCTN2 siRNA

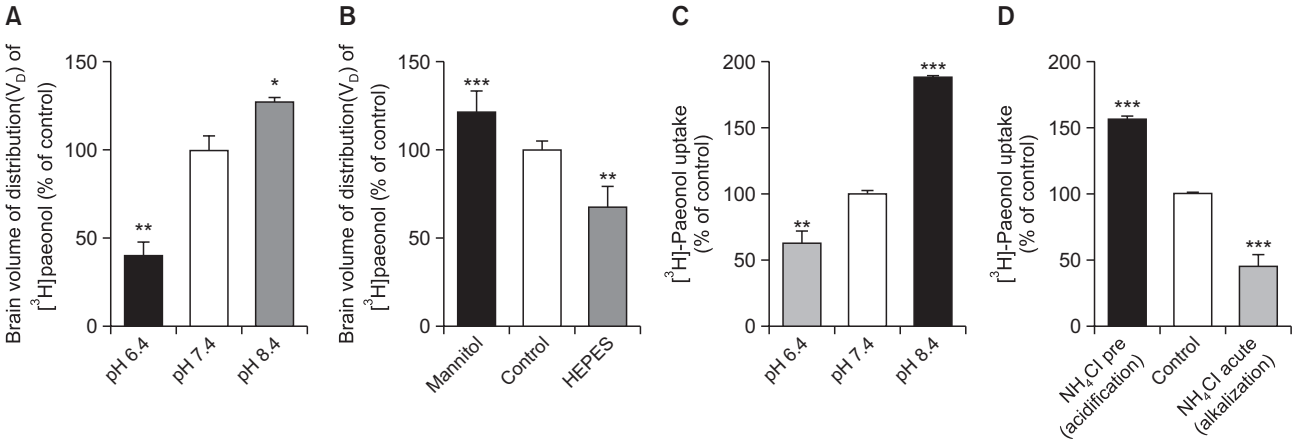

Fig. 3. Effect of changed extracellular (A) and intracellular (B) pH on [^{3}H]paeonol transport in rat brain by using ICAP at rate of 4 mL/min for 15 s. Effect of changed extracellular (pH_e) (C) and intracellular (pH_i) (D) pH on [^{3}H]paeonol uptake by TR-BBB cells was determined for 5 min at 37°C. Each point represents the mean ± SEM (n=3-4). *p<0.05, **p<0.01, ***p<0.001 compared to the control at pH 7.4.

and rPMAT siRNA or control siRNA at concentration 200 nM using Lipofectamine® 2000 transfection reagent (Invitrogen, Carlsbad, CA, USA) according to the manufacturer's protocol. Cells were incubated at 33°C for 48 h in a CO_2 incubator. Knockdown of these transporters were checked by real-time PCR. Uptake of [^{3}H]peaonol (13.9 nM) for 5 min or [^{3}H]ALC (1.67 nM) and [^{3}H]MPP^+ (1.19 nM) for 15 min was measured as described above.

Statistical data analysis

All data are expressed as mean ± standard error of mean (SEM). Data were subjected to one-way analysis of variance (ANOVA) with Dunnett's (post hoc test). Differences were considered statically significant at p<0.05.

RESULTS

In vivo blood-to-brain transport of [^{3}H]paeonol and pharmacokinetics in rats

First, brain uptake of [^{3}H]paeonol across the BBB *in vivo* was investigated following IV injection in rats. Pharmacokinetic parameters of [^{3}H]paeonol, unlabeled paeonol 10 mM and pyrilamine 10 mM were estimated from the plasma concentration-time profile shown in (Fig. 1A) using non-compartmental pharmacokinetic analysis. Similarly, the area under the plasma concentration-time curve (AUC) of paeonol 10 mM (25.7 ± 2.7) and pyrilamine 10 mM (35.0 ± 5.3) were increased significantly compared to the control (18 ± 1.7). In addition, the brain uptake (%ID/g) of the plasma parameter of [^{3}H]paeonol with unlabeled paeonol of concentration 10 mM (0.012 ± 0.001) and pyrilamine 10 mM (0.020 ± 0.023) were increased compared to the control (0.0087 ± 0.0007) but the PS products did not show any difference in the normal SD rats (Fig. 1B). Pharmacokinetic parameters of [^{3}H]paeonol and other compounds are summarized in Table 1. The terminal half-life ($T_{1/2}$) of [^{3}H]paeonol with the addition of cold paeonol 10 mM was increased compared to control but the $V_{d,ss}$ (mL/kg) has no any differences. Similarly, the clearance CL of [^{3}H]paeonol with the addition of cold pyrilamine and paeonol were significantly decreased but the MRT (min) was increased in the rats (Table 1). As shown in Table 2, the volume of distribution (V_D) of [^{3}H]paeonol by the rat brain was about 6-fold higher than that of sucrose, the vascular space marker of BBB (Bickel *et al*., 1996). Moreover, the %ID/g of [^{3}H]paeonol uptake by the brain and kidney showed significant increase in the presence of paeonol and pyrilamine of concentration 10 mM but by heart, liver and lungs did not show any difference during the uptake (Fig. 1B, Table 2). *In vivo* pharmacokinetic results indicated that paeonol could actively transport across the BBB under physiological state.

In vivo concentration dependence of [^{3}H]paeonol transport

To measure BBB permeability and changes of concentration of paeonol to the brain transport through BBB, [^{3}H]paeonol transport was measured following the ICAP method. The initial transport of [^{3}H]paeonol in rat brain was plotted against the total paeonol concentration. Both saturable component (Michaelis-Menten) and unsaturable component are shown in Fig. 2A. The uptake of [^{3}H]paeonol was found to be concentration dependent with the K_m of 0.28 mM, V_{max} of 1.05 μmol/min/g of the brain and the K_d value was 0.41 μmol/min/g (Fig. 2A). Passive diffusion accounted for 17% of the total brain uptake of [^{3}H]paeonol while carrier-mediated influx was responsible for 83% of the total brain uptake of [^{3}H]paeonol. These results suggested that paeonol could be transported by carrier-mediated transporter at the BBB.

Effect of several compounds on [^{3}H]paeonol transport in rat brain *in vivo*

The inhibitory effect of several compounds on the transport of [^{3}H]paeonol was determined. The values of V_D of [^{3}H] paeonol are shown in (Table 3) using the ICAP method. The uptake of paeonol was strongly inhibited by pyrilamine, diphenhydramine, and tramadol. The uptake of paeonol was also showed significantly reduction effects by paeonol, imperatorin, MPP^+ (PMAT inhibitor), ALC (an OCTN2-specific substrate), verapamil, and quinidine (organic cations). However, the uptake of [^{3}H]paeonol was not affected by choline (choline like transporter, CTL1 substrate), TEA (OCT substrate), or 6-mercaptopurine (6-MP) OATP1, OATP3, MRP4, and MRP5

Table 5. Effect of ATP-depletion, sodium replacement, membrane potential and protonophore (proton gradient) on [^{3}H]paeonol uptake by TR-BBB cells

Treatment	Relative uptake (% of control)
Control	100 ± 4
Sodium azide (0.1%)	56 ± 8**
FCCP (10 μM)	67 ± 1***
NMG^+	91 ± 0.9
Valinomycin (10 μM)	103 ± 3
KCl	97 ± 4

The [^{3}H]paeonol uptake was measured at 37°C for 5 min with metabolic inhibitors as 0.1% sodium azide (NaN_3) to deplete ATP. Sodium in transport buffer was replaced by with *N*-methyglucamine$^+$ (NMG^+). Potassium (K), valinomycin and 10 μM carbonyl cyanide-*p*-trifluoromethoxyphenylhydrazone (FCCP) was pretreated to disrupt membrane potential (KCl) and to disrupt proton gradient, respectively. Each point represents the mean ± SEM (n=3-4), pH 7.4. ** p<0.01, *** p<0.001 was significantly different from control.

substrate compared to the control (Table 3). These results suggest that the transport of [^{3}H]paeonol involves a carrier-mediated process.

In vivo blood-to-brain transport of [^{3}H]paeonol across BBB

The carotid artery single injection technique showed that the BUI value of [^{3}H]paeonol was decreased more than 60 % in the presence of paeonol 10 mM (Table 4). Similarly, other cationic compounds such as verapamil, tramadol, imperatorin, clonidine, pyrilamine, propranolol and nicotine also showed significant reduction effect in BUI study. In contrast, TEA, PAH, choline and taurine did not express any significant effect in BUI of [^{3}H]paeonol.

Effect of extracellular and intracellular pH on [^{3}H]paeonol uptake in rat brain

Alteration of extracellular pH (pH_e): The effect of pH_e on [^{3}H]paeonol uptake in rat brain *in vivo* was investigated. The uptake of paeonol was significantly decreased at acidic pH (6.4) but, increased at alkaline pH 8.4 compared to that at pH 7.4 (Fig. 3A).

Alteration of intracellular pH (pH_i): Rat brain was perfused with [^{3}H]paeonol in KHB buffer containing mannitol (acidification) which revealed that the uptake was significantly increased compared to the control. In contrast, when sodium free-KHB buffer with the addition of HEPES (for alkalization of the extracellular pH), the uptake of paeonol was significantly decreased by brain endothelial cells compared to the control (Fig. 3B).

Characteristics of transport mechanism of [^{3}H]paeonol by TR-BBB cells

To clarify the transport mechanism/function of [^{3}H]paeonol by TR-BBB cells, we have used an *in vitro* method. The uptake of [^{3}H]paeonol was carried out in the presence of various concentrations (0-1 mM) of unlabeled paeonol. Data of kinetic parameters (K_m and V_{max}) were fitted by Michaelis-Menten equation and result are shown in (Fig. 2B). Kinetic analysis of paeonol uptake revealed a high-affinity K_{m1} value of 17 μM, a low-capacity V_{max1} of 0.0721 nmol/mg protein/min, a low-affinity K_{m2} value of 2.10 mM, and a high-capacity V_{max2} of 7.89 nmol/mg protein/min in the BBB. The inset graph as shown in Fig. 2B represents the high affinity and low capacity at the concentration range of 0-0.25 mM.

Table 6. Effect of various compounds transporter inhibitor on [^{3}H]paeonol uptake at 5 min into TR-BBB cells

Inhibitor	Concentration (mM)	% Of control uptake	Predicted Log D
Control		100 ± 2	
Paeonol	1	45 ± 5.0***	2.31
Tramadol	1	29 ± 7**	0.29
Pyrilamine	1	52 ± 3***	0.76
Diphenhydramine	1	75 ± 0.3***	3.43
Imperatorin	1	74 ± 3**	4.01
	2	45 ± 8**	
Dopamine	1	61 ± 0.1***	–2.18
MPP+	1	75 ± 3*	–0.29
ALC	1	79 ± 3**	–3.69
Verapamil	1	77 ± 2**	2.46
Quinidine	1	77 ± 2***	0.98
TEA	1	99 ± 6	–3.26
Choline	1	122 ± 20	–4.14
E.S	1	105 ± 6	–1.4
PAH	1	108 ± 7	–3.69
6-MP	1	102 ± 4	–3.09

ALC, acetyl-L-carnitine; E.S, estrone 3-sulfate; TEA, tetraethylammonium; PAH, para-aminohippuric acid. MPP^+, 1-methyl-4-phenylpyridinium; 6-MP, 6-mercaptopurine. Uptake of [^{3}H]paeonol was measured at 37°C for 5 min in the transport ECF buffer (pH 7.4) that containing each 1-2 mM of compound. The cellular uptake is presented as percent of control. The data of each value represent the mean ± SEM (n=3-4). * p<0.05, ** p<0.01, *** p<0.001 was significantly different from control pH: 7.4.

The effects of paeonol uptake on ATP depletion, membrane potential disruption, proton gradient, and sodium replacement was investigated by TR-BBB cells. The uptake of [^{3}H]paeonol was significantly decreased by the pretreatment of sodium azide (0.01% metabolic inhibitor) and 10 μM of FCCP, a protonophore. However, the uptake was not change by the replacement of extracellular sodium ion with N-methylglucamine, potassium chloride, or by pre-treatment with valinomycin compared to that in the control (Table 5). [^{3}H]Paeonol uptake was decreased and increased significantly at extracellular pH 6.4, and pH 8.4 compared to the control pH 7.4 (Fig. 3C) respectively. In addition, the uptake was markedly increased at acidic pH_i and depleted at alkalized pH_i (Fig. 3D). These results showed that [^{3}H]paeonol uptake was concentration, energy and pH dependent but it was independent of membrane potential or sodium ion.

Inhibitory effect of several compounds on [^{3}H]paeonol uptake by TR-BBB cells

To characterize the transport mechanism of paeonol by TR-BBB cells, inhibitory effect of several compounds was investigated. As shown in Table 6, the uptake of [^{3}H]paeonol was inhibited by tramadol, pyrilamine, diphenhydramine, quinidine, verapamil, MPP^+, dopamine, and ALC. In contrast, TEA, choline, PAH, E.S, and 6-MP had no significant effect on paeonol uptake by TR-BBB cells (Table 6). Therefore, the uptake was mediated by a carrier mediated transporter system.

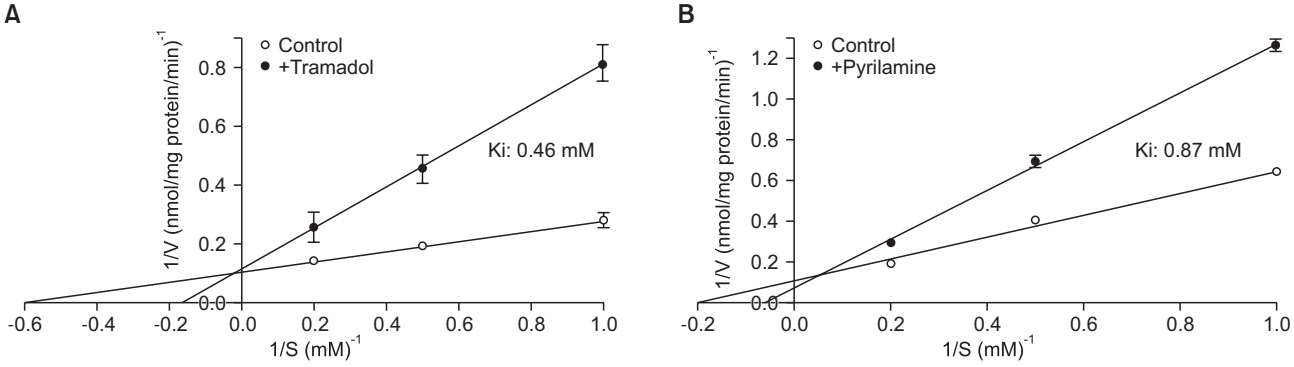

Fig. 4. Lineweaver-Burk plot analysis of [^{3}H]paeonol uptake with tramadol and pyrilamine into TR-BBB cells. [^{3}H]Paeonol uptake (1, 2, and 5 mM for 5 min) was measured in the absence (○) or presence (●) of 2 mM of tramadol and pyrilamine in TR-BBB cells. Each point represents the mean ± SEM of three determinations.

Inhibitory effects of other compounds on [^{3}H]paeonol uptake by TR-BBB cells

To determine whether the carrier mediated transporter system accepts paeonol as a substrate, we examined the mutual inhibitory effects on 2 mM of tramadol and pyrilamine uptake by [^{3}H]paeonol on TR-BBB cells. Lineweaver-Burk plot analysis indicated that there was competitive inhibition effect in the presence of tramadol and pyrilamine with the K_i values of 0.46 mM and 0.87 mM respectively on [^{3}H]paeonol uptake (Fig. 4).

Effect of rOCTN2 and rPMAT siRNA transfection on [^{3}H]paeonol uptake by TR-BBB cells

To determine whether OCTN2 and rPMAT were involved in [^{3}H]paeonol uptake by TR-BBB cells, OCTN2 and rPMAT siRNA transfection were used for the knocked out study. The mRNA expression levels of rOCTN2 and rPMAT in BBB cells were determined by quantitative RT-PCR (data not shown). Both [^{3}H]ALC and [^{3}H]MPP$^+$ uptake were significantly decreased by OCNT2 and rPMAT siRNA transfected cells compared to the control (Fig. 5A, 5B). In contrast, [^{3}H]paeonol uptake was not affected by the rOCTN2 and rPMAT siRNA transfected (Fig. 5C, 5D). These results suggest that OCTN2 and rPMAT are not involved in the uptake of [^{3}H]paeonol by TR-BBB cells.

Comparison of inhibitory effect and lipophilicity of compounds on the uptake of [^{3}H]paeonol

To examine the relationship between the inhibitory effect and lipophilicity of compounds on the uptake of [^{3}H]paeonol in rat brain *in vivo* and *in vitro*, relative inhibition [100-relative brain uptake (%)] and log n-octanol-ringer distribution coefficient at pH 7.4 called log D were calculated following previous reports (Kubo *et al*., 2013b). Results are shown in (Fig. 6A, 6B) and (Table 3, 6). The plotted cationic compounds were separately classified into group I-II after comparing the relative inhibition and lipophilicity of brain distribution volume (V_D) in rats. Both group I (tramadol, pyrilamine, quinidine, MPP+, diphenhydramine) and group II (choline, TEA, and ALC) compounds had significant inhibition effects on [^{3}H]paeonol uptake except choline and TEA. Group III is type of organic anion compounds, they had no significant effect on [^{3}H]paeonol uptake (Fig. 6B) using regression line estimated with equation 12. The star mark represented strong inhibition effect of unlabeled paeonol on the uptake of [^{3}H]paeonol. Regression line for the entire groups of compounds was estimated using the following equation:

$$\text{Relative inhibition (\%) of } V_D = 7.02 \times \log D + 29.5 \quad (12)$$

$$\text{Relative inhibition (\%)} = 5.88 \times \log D + 25.3 \quad (13)$$

DISCUSSION

Paeonol has reputed broad range of neuroprotective effect in various models of CNS disorders such as ischemic stroke, diabetic encephalopathy (DE), AD as well as the counteraction of neurological disorders (Liu *et al*., 2013; Zhao *et al*., 2014). Pharmacokinetic study is effective to predict the efficacy, toxicity and clinical applications of the compounds (Xie *et al*., 2008). Distribution of paeonol and its metabolite to brain is very high by oral administration (Li *et al*., 2012). However, the transport mechanism of paeonol has not been clearly identified across the BBB. So, we pursue to investigate the brain uptake, pharmacokinetic and permeability of paeonol by using an internal carotid artery perfusion method in brain.

In the present study, changes in the pharmacokinetics and the brain distribution of [^{3}H]paeonol with the addition of other compounds (unlabeled pyrilamine and paeonol 10 mM) was investigated in order to determine the metabolic profile of paeonol. Pharmacokinetic parameters of [^{3}H]paeonol after IV injection are shown in (Fig. 1, Table 1, 2). Pharmacokinetic parameters such as AUC (%ID*min/mL) and %ID/g value of [^{3}H]paeonol presents the marked induction in the presence of cold paeonol and pyrilamine at a concentration of 10 mM. In contrast, the PS (μL/min) value had no any effect in the rat brain (Fig. 1B). [^{3}H]Paeonol uptake with the addition of the other compounds shows significantly higher in the half- life ($T_{1/2}$), AUC, MRT and the %ID/g profile but the PS product has no effect in the rat brain. However, the CL was decreased significantly with the addition of compounds and the $V_{d.ss}$ value has decreased only in the pyrilamine addition. Brain volume of distribution (V_D) of [^{3}H]paeonol was about 6-fold higher than that of sucrose (Bickel *et al*., 1996) and the V_D was markedly reduced during the addition of compounds. Similarly, the uptake of [^{3}H]paeonol (0.0087 %ID/g) was similar to that of [^{3}H] paclitaxel (0.010 %ID/g) but it was 3 fold greater than that of [^{3}H]morphine-6-glucuronide (0.0026 %ID/g) but other organs such as heart, liver and lung has no difference (Wu *et al*.,

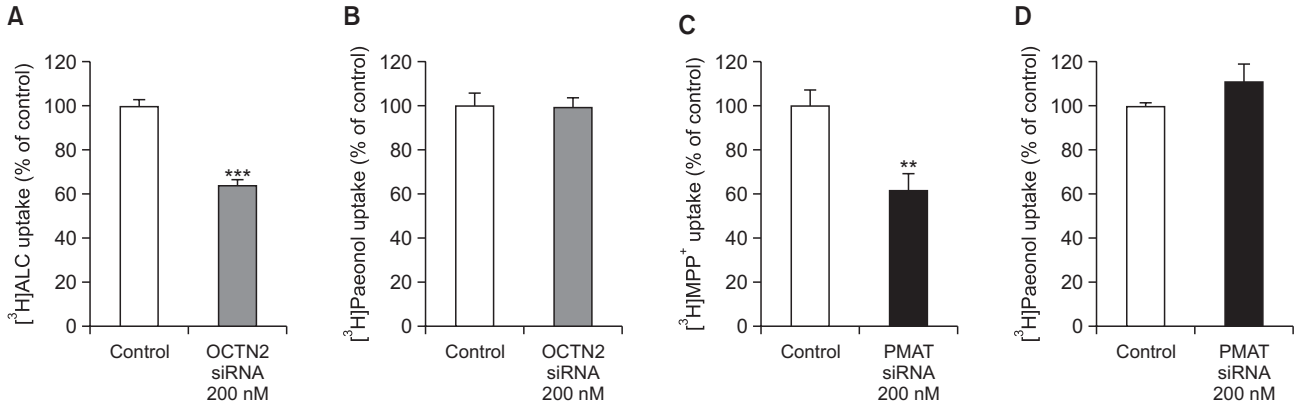

Fig. 5. Effect of OCTN2 siRNA on uptake of [^{3}H]ALC and [^{3}H]paeonol (A) and the effect of rPMAT siRNA on uptake of [^{3}H]MPP$^+$ and [^{3}H]paeonol (B) by TR-BBB cells. Cells were transfected with negative control, OCTN2 siRNA, or rPMAT siRNA using Lipofectamine 2000 transfection reagent. After 2 days of transfection, the uptakes of [^{3}H]ALC and [^{3}H]MPP$^+$ were measured at 15 min and the uptake of [^{3}H]paeonol was measured at 37°C for 5 min. Each point represents mean ± SEM of three or four determinations at pH 7.4. ***p*<0.01 compared to the control.

1997; Lee *et al*., 2014b). Moreover, the V_D of [^{3}H]paeonol in rat brain following ICAP technique was 67 fold greater than the V_D of [^{14}C]sucrose (Pardridge *et al*., 1994) (Table 1, 2). These finding are consistent with the current studies. Paeonol is highly lipid soluble compound and has a low molecular weight so it can be expected that it can cross the BBB under the physiological state. Our results also proved that paeonol has high BBB permeability. In general, it has widely been known that the changes in the pharmacokinetic parameter might not alter the drug efficacy in non-linear pharmacokinetics (Lee *et al*., 2014b).

Our *in vivo* results revealed that brain transport of [^{3}H]paeonol was in a concentration dependent manner (Fig. 2A). The apparent Michaelis-Menten (K_m) of paeonol parameter was 0.28 mM in the brain. Similarly, the K_m value of clonidine was 0.62 mM (Andre *et al*., 2009). *In vivo* carrier-mediated transport rate was about 3.8 μL/min/g and passive transport rate was about 0.4 μL/min/g. The influx rate of paeonol was 9 times more than its passive diffusion when its concentration was less than the apparent K_m value. To identify the transport system of paeonol involved in rat brain, the effects of various compounds on paeonol uptake were determined (Table 3, 4). [^{3}H]Paeonol uptake by rat brain was significantly decreased by the substrates of the novel organic cationic compounds such as imperatorin, tramadol, pyrilamine, nicotine, verapamil, propranolol, clonidine and diphenhydramine (Okura *et al*., 2008; Kubo *et al*., 2013a; Kitamura *et al*., 2014; Tega *et al*., 2015a, 2015b; Tun and Kang, 2017). It was also significantly inhibited by MPP$^+$ (Okura *et al*., 2011) and ALC (Lee *et al*., 2012). However, there was no effect by OCTs & OCTN1 substrate (TEA) (Tamai *et al*., 2004; Ohtsuki and Terasaki, 2007; Chapy *et al*., 2014) CTL1 substrate (choline) (Lee and Kang, 2010), OATP1-3, or MRP4 & 5 inhibitor (6-MP) (Mori *et al*., 2004; Hosoya *et al*., 2009; Lee *et al*., 2011) (Table 3, 4).

Paeonol uptake was found to be concentration-dependent with the K_{m1}, K_{m2}, V_{max1} and V_{max2} values of 17 μM, 2.10 mM and 0.072 nmol/mg/protein/min and 7.88 nmol/mg/protein, respectively (Fig. 2B). A kinetic analysis revealed that saturable component (V_{max}/K_m) was in the lower concentration range (<0.25 mM) in TR-BBB cells. The inset graph (Fig. 2B) represents the higher affinity and lower capacity than the outside graph of Fig. 2B.This result is similar to the pyrilamine (organic cationic) influx system also expressing the high- and low- affinity transport processes at BBB with K_{m1} of 20 μM and K_{m2} of 252 μM (Kubo *et al*., 2013a). Both *in vivo* and *in vitro* results provides evidence that carrier mediated and novel organic cationic transporter system mediated for paeonol transport to the brain. Paeonol uptake was significantly increased and decreased at extracellular pH 8.4 and 6.4 respectively (Fig. 3A). Similarly, the effect of intracellular pH on paeonol uptake reduced at alkalization but increased at acidification (Fig. 3B). The detail mechanisms of paeonol transport across the BBB was expressed by *in vitro* cellular uptake study in TR-BBB cells. *In vivo* and *in vitro* results are expressed in the same patterns (Fig. 3C, 3D). Moreover, the uptake of [^{3}H]paeonol was significantly reduced with the pre-treatment of metabolic inhibitor (NaN_3) and FCCP (protophore). However, the uptake was not dependent on sodium and membrane potential but dependent with pH and energy (Table 5). *In vivo* and *in vitro* results are expressed in the same patterns (Fig. 3C, 3D). The paeonol uptake results are similar to those reported in previous studies which expressed the proton coupled organic cationic antiporter system involved for the functional transport of several compounds such as tramadol, pyrilamine, diphenhydramine and oxycodone (Okura *et al*., 2008; Sadiq *et al*., 2011; Shimomura *et al*., 2013; Kitamura *et al*., 2014; Tun and Kang, 2017).

In vitro inhibition result is similar to the *in vivo* result as shown in (Table 3, 4, 6). Most substrates of the organic cation transporter/carrier mediated transporter have amine attached to an aromatic moiety through an appropriate length of linker but peonol is distinguish differently than these substrates. However, [^{3}H]paeonol uptake was inhibited the substrates of novel OCT (tramadol, diphenhydramine, pyrilamine), OCTN2 (ALC) and PMAT (MPP$^+$) but not the MATE and OCTN1 substrate (TEA). From here we have selected two compounds tramadol and pyrilamine for the [^{3}H]paeonol competitive inhibition study. The uptake of [^{3}H]paeonol was competitively inhibited by those compounds (Fig. 4A, 4B). The Ki value is related to the percentage of inhibition study. They have mutually inhibited the uptake of paeonol suggesting that the paeonol can transport to the BBB similar to the tramadol and pyrilamine,

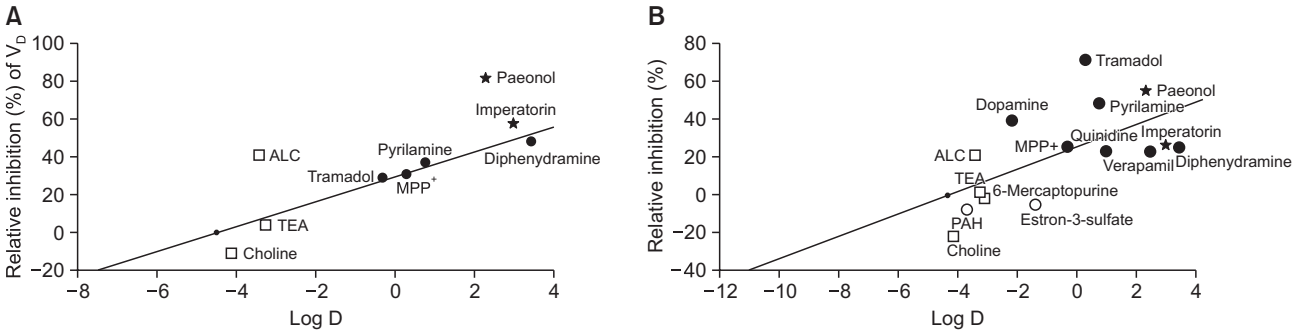

Fig. 6. A comparison of inhibitory effect and lipophilicity. (A) Relative inhibition of VD on rat brain and (B) relative inhibition on TR-BBB cells were compared for compounds with different lipophilicity. The relative inhibition [100-relative uptake (%)] was calculated based on the value listed in Table 3 and 4. Compounds were classified as group I [*closed circles*: primary, secondary, tertiary amines, and *closed star* (paeonol and imperatorin)], group II (open squares: quaternary ammonium cations, group III (open circles: PAH and estron-3-sulfate), and organic anion substrates (OAT3 and Oatps). The regression lines of these groups are described by equation 11 and 12 in panels (A) and (B), respectively.

those follows the novel organic cationic transporter system.

Inhibition study (Table 3, 4, 6) data presents inhibitory characteristics are partially consistent with those of the organic cationic transporter/system at the blood brain barrier. Novel organic cationic transporter substrate such as pyrilamine, tramadol, diphenhydramine and verapamil, and OCTN2 substrate ALC, PMAT substrate MPP^+ showed the reduction effects in the uptake of paeonol. In addition, OCTN1/MATE transporter substrate TEA had no effect on the uptake study. Therefore, we were curious to investigate which transporter system mainly involved for the paeonol transport at BBB. Taking reference as inhibition results, we have selected PMAT and OCTN2 because ALC and MPP+ has presented for inhibition but TEA not in the paeonol uptake. Furthermore, to determine whether OCTN2, PMAT or other transporter system involved for paeonol uptake SiRNA transfection and uptake study was done in the BBB cell lines. The known transporters such as OCTN2 (ALC) and PMAT (MPP^+) siRNA transfected cells shows the significant reduction effect with the corresponding uptake. Similarly to identify the [^{3}H]paeonol transporter system, same SiRNAs were used for the transfection of the cells but the uptake was carried out by [^{3}H]paeonol. The observed results expressed that OCTN2 and PMAT did not contribute for the transport of paeonol to the BBB. So, it concludes novel organic cationic transporter system involved for the paeonol uptake in BBB (Fig. 5) (Higuchi *et al*., 2015).

Furthermore, the inhibitory effects of cationic compounds with different lipophilicity were compared in order to investigate the interaction of cations and paeonol influx system at BBB. Both group I (tramadol, pyrilamine, quinidine, MPP^+ and diphenhydramine) and group II (choline, TEA and ALC) compounds had significant inhibition effects on [^{3}H]paeonol uptake except choline and TEA suggesting that the paeonol influx system could be significantly inhibited by lipophilic amines due to the relationship between relative inhibition and predicted log D (Kubo *et al*., 2013b). Moreover, high relative inhibition value by unlabeled paeonol supports the hypothesis that paeonol can undergoes specific carrier-mediated transporter system (Fig. 6A). Results of *in vitro* inhibitory effect of lipophilic amines on paeonol uptake were similar to *in vivo* results (Fig. 6B). Especially, tramadol, pyrilamine, ALC and dopamine showed high relative inhibitory effect on paeonol uptake. These results suggest that the paeonol influx system can effectively recognize lipophilic amines such as drug (nicotine, memantine and apomorphine etc.) used for treating CNS disorders (Tega *et al*., 2013; Okura *et al*., 2014b; Higuchi *et al*., 2015). And [^{3}H]paeonol transport in rat BBB could be related to novel organic cationic transporter system.

Based on our *in vitro* and *in vivo* results, [^{3}H]paeonol uptake is dependent on concentration, pH and energy. It is inhibited by substrates of the carrier mediated and organic cationic transporter system. [^{3}H]Paeonol permeability to cross the BBB is high and for the transport across the BBB involves the carrier mediated transporter system. For the future aspects, paeonol can be a good candidate not only for the prevention of CNS disorders but also in the development of new CNS-acting drugs for human beings.

ACKNOWLEDGMENTS

The authors thank to Temdara Tun for helping *in vitro* experiments, also thankful to Dr. T. Terasaki providing us the TR-BBB cells. We are grateful to Dong-A Pharmaceutical Co., Ltd., for providing the paeonol and other plant extract. This research was supported by a grant (No. 2011-0030074) of the National Research Foundation of Korea (NRF) funded by the Ministry of Science, ICT and Future Planning (MSIP), Republic of Korea.

REFERENCES

Abbott, N. J., Patabendige, A. A., Dolman, D. E., Yusof, S. R. and Begley, D. J. (2010) Structure and function of the blood-brain barrier. *Neurobiol. Dis.* **37**,13-25.

Andre, P., Debray, M., Scherrmann, J. M. and Cisternino, S. (2009) Clonidine transport at the mouse blood-brain barrier by a new H^+ antiporter that interacts with addictive drugs. *J. Cereb. Blood Flow Metab.* **29**, 1293-304.

Bickel, U., Schumacher, O. P., Kang, Y. S. and Voigt, K. (1996) Poor permeability of morphine 3-glucuronide and morphine 6-glucuronic through the blood-brain barrier in the rat. *J. Pharmacol. Exp. Ther.* **278**,107-113.

Boström, E., Simonsson, U. S. and Hammarlund-Udenaes, M. (2006) In vivo blood-brain barrier transport of oxycodone in the rat: indica-

tions for active influx and implications for pharmacokinetics/pharmacodynamics. *Drug Metab. Dispos.* **34**, 1624-1631.
Chapy, H., Smirnova, M., André, P., Schlatter, J., Chiadmi, F., Couraud, P. O., Scherrmann, J. M., Declèves, X. and Cisternino, S. (2014) Carrier-mediated cocaine transport at the blood-brain barrier as a putative mechanism in addiction liability. *Int. J. Neuropsychopharmacol.* **18**, 1-10.
Cisternino, S., Chapy, H., Andre, P., Smirnova, M., Debray, M. and Scherrmann, J. M. (2013) Coexistence of passive and proton antiporter-mediated processes in nicotine transport at the mouse blood-brain barrier. *AAPS J.* **15**, 299-307.
Higuchi, K., Kitamura, A., Okura, T. and Deguchi, Y. (2015) Memantine transport by a proton-coupled organic cation antiporter in hCMEC/D3 cells, an *in vitro* human blood-brain barrier model. *Drug Metab. Pharmacokinet.* **30**, 182-187.
Himaya, S. W., Ryu, B., Qian, Z. J. and Kim, S. K. (2012) Paeonol from Hippocampus kudaBleeler suppressed the neuro-inflammatory responses *in vitro* via NF-κB and MAPK signaling pathways. *Toxicol. In Vitro.* **26**, 878-887.
Hosoya, K., Makihara, A., Tsujikawa, Y., Yoneyama, D., Mori, S., Terasaki, T., Akanuma, S., Tomi, M. and Tachikawa, M. (2009) Roles of inner blood-retinal barrier organic anion transporter 3 in the vitreous/retina-to-blood efflux transport of p-aminohippuric acid, benzylpenicillin, and 6-mercaptopurine. *J. Pharmacol. Exp. Ther.* **329**, 87-93.
Kang, Y. S., Boado, R. J. and Pardrodge, W. M. (1995) Pharmacokinetic and the organ clearance of A 3'-Biotinylaed, internally [^{32}P]-labeled phosphodiester oligodeoxynucleotide coupled to a neutral avidin/monoclonal antibody conjugate. *Drug. Metab. Dispos.* **23**, 55-59.
Kang, Y. S. and Park, J. H. (2000) Brain uptake and the analgesic effect oxytocin its usefulness as an analgesic agent. *Arch. Pharm. Res.* **23**, 391-395.
Kang, Y. S., Lee, K. E., Lee, N. Y. and Terasaki, T. (2005) Donepezil tacrine and alpha-Phenyl-n-tert-Butyl nitrone (PBN) inhibit choline transport by conditionally immortalized rat brain capillary endothelial cell line (TR-BBB). *Arch. Pharm. Res.* **28**, 443-450.
Kang, Y. S., Ohtsuki, S., Takanaga, H., Tomi, M., Hosoya, K. and Terasaki, T. (2002) Regulation of taurine transport at the blood-brain barrier by tumor necrosis factor-alpha, taurine and hypertonicity. *J. Neurochem.* **83**, 1188-1195.
Kitamura, A., Higuchi, K., Okura, T. and Deguchi, Y. (2014) Transport characteristics of tramadol in the blood-brain barrier. *J. Pharm. Sci.* **103**, 3335-3341.
Kooijmans, S. A., Senyschyn, D., Mezhiselvam, M. M., Morizzi, J., Charman, S. A., Weksler, B., Romero, I. A., Couraud, P. O. and Nicolazzo, J. A. (2012) The involvement of a Na^+- and Cl^--dependent transporter in the brain uptake of amantadine and rimantadine. *Mol. Pharm.* **9**, 883-893.
Kubo, Y., Kusagawa, Y., Tachikawa, M., Akanuma, S. and Hosoya, K. (2013a) Involvement of a novel organic cation transporter in verapamil transport across the inner blood-retinal barrier. *Pharm. Res.* **30**, 847-856.
Kubo, Y., Shimizu, Y., Kusagawa, Y., Akanuma, S. and Hosoya, K. (2013b) Propranolol transport across the inner blood-retinal barrier: potential involvement of a novel organic cation transporter. *J Pharm. Sci.* **102**, 3332-3342.
Lau, C. H., Chan, C. M., Chan, Y. W., Lau, K. M., Lau, T. W., Lam, F. C., Law, W. T., Che, C. T., Leung, P. C., Fung, K. P., Ho, Y. Y. and Lau, C. B. (2007) Pharmacological investigations of the antidiabetic effect of Cortex Moutan and its active component paeonol. *Phytomedicine* **14**, 778-784.
Lee, N. Y. and Kang, Y. S. (2010) The inhibitory effect of rivastigmine and galantamine on choline transport in brain capillary endothelial cells. *Biomol. Ther. (Seoul)* **18**, 65-70.
Lee, N. Y. and Kang, Y. S. (2016) *In vivo* and *in vitro* evidence for brain uptake of 4-Phenylbutyrate by the monocarboxylate transporter 1 (MCT1). *Pharm. Res.* **33**, 1711-1722.
Lee, N. Y., Choi, H. O. and Kang, Y. S. (2012) The acetylcholinesterase inhibitors competitively inhibited an acetyl L-carnitine transport through the blood-brain barrier. *Neurochem. Res.* **37**, 1499-1507.
Lee, N. Y., Lee, H. E. and Kang, Y. S. (2014a) Identification of P-Glycoprotein and transport mechanism of Paclitaxel in syncytiotrophoblast cells. *Biomol. Ther. (Seoul)* **22**, 68-72.
Lee, N. Y., Lee, K. B. and Kang, Y. S. (2014b) Pharmacokinetic, placenta, and brain uptake of paclitaxel in pregnant rats. *Cancer Chemother. Pharmacol.* **73**, 1041-1045.
Lee, N. Y., Sai, Y., Nakashima, E., Ohtsuki, S. and Kang, Y. S. (2011) 6-Mercaptopurine transport by equilibrative nucleoside transporters in conditionally immortalized rat syncytiotrophoblast cell lines TR-TBTs. *J. Pharm. Sci.* **100**, 3773-3782.
Li, H., Wang, S., Zhang, B., Xie, Y., Wang, J., Yang, Q., Cao, W., Hu, J. and Duan, L. (2012) Influence of co-administered danshensu on pharmacokinetic fate and tissue distribution of paeonol in rats. *Planta Med.* **78**, 135-140.
Lin, H. C., Ding, H. Y., Ko, F. N., Teng, C. M. and Wu, Y. C. (1999) Aggregation inhibitory activity of minor acetophenones from Paeonia species. *Planta Med.* **65**, 595-599.
Liu, J., Feng, L., Ma, D., Zhang, M., Gu, J., Wang, S., Fu, Q., Song, Y., Lan, Z., Qu, R. and Ma, S. (2013) Neuroprotective effect of paeonol on cognition deficits of diabetic encephalopathy in streptozotocin-induced diabetic rat. *Neurosci. Lett.* **549**, 63-68.
Misra, A., Ganesh, S., Shahiwala, A. and Shah, S. P. (2003) Drug delivery to the central nervous system: a review. *J. Pharm. Sci.* **6**, 252-273.
Mori, S., Ohtsuki, S., Takanaga, H., Kikkawa, T., Kang, Y. S. and Terasaki, T. (2004) Organic anion transporter 3 is involved in the brain-to-blood efflux transport of thiopurine nucleobase analogs. *J. Neurochem.* **90**, 931-941.
Ohtsuki, S. and Terasaki, T. (2007) Contribution of carrier-mediated transport systems to the blood-brain barrier as a supporting and protecting interface for the brain; importance for CNS drug discovery and development. *Pharm. Res.* **24**, 1745-1758.
Okura, T., Hattori, A., Takano, Y., Sato, T., Hammarlund-Udenaes, M., Terasaki, T. and Deguchi, Y. (2008) Involvement of the pyrilamine transporter, a putative organic cation transporter, in blood-brain barrier transport of oxycodone. *Drug Metab. Dispos.* **36**, 2005-2013.
Okura, T., Kato, S., Takano, Y., Sato, T., Yamashita, A., Morimoto, R., Ohtsuki, S., Terasaki, T. and Deguchi, Y. (2011) Functional characterization of rat plasma membrane monoamine transporter in the blood-brain and blood-cerebrospinal fluid barriers. *J. Pharm. Sci.* **100**, 3924-38.
Okura, T., Higuchi, K., Kitamura, A. and Deguchi, Y. (2014a) Proton-coupled organic cation antiporter-mediated uptake of apomorphine enantiomers in human brain capillary endothelial cell line hCMEC/D3. *Biol. Pharm. Bull.* **37**, 286-291.
Okura, T., Kato, S. and Deguchi, Y. (2014b) Functional expression of organic cation/carnitine transporter 2 (OCTN2/SLC22A5) in human brain capillary endothelial cell line hCMEC/D3, a human blood-brain barrier model. *Drug Metab. Pharmacokinet.* **29**, 69-74.
Palmer, A. M. (2011) Neuroprotective therapeutics for Alzheimer's disease. *Trends Pharmacol. Sci.* **32**, 141-147.
Pardridge, W. M., Kang, Y. S. and Buciak, J. L. (1994) Transport of human recombinant brain-derived neurotrophic factor (BDNF) through the rat blood-brain barrier *in vivo* using vector-mediated peptide drug delivery. *Pharm. Res.* **11**, 738-746.
Pardridge, W. M. (2005) The blood-brain barrier: bottleneck in brain drug development. *NeuroRx* **2**, 3-14.
Pardridge, W. M. (2012) Drug transport across the blood-brain barrier. *J. Cereb. Blood Flow Metab.* **32**, 1959-72.
Pardridge, W. M. (2015) Blood-brain barrier endogenous transporters as therapeutic targets: a new model for small molecule CNS drug discovery. *Expert. Opin. Ther. Targets* **19**, 1059-1072.
Sadiq, M. W., Borgs, A., Okura, T., Shimomura, K., Kato, S., Deguchi, Y., Jansson, B., Björkman, S., Terasaki, T. and Hammarlund-Udenaes, M. (2011) Diphenhydramine active uptake at the blood-brain barrier and its interaction with oxycodone *in vitro* and *in vivo*. *J. Pharm. Sci.* **100**, 3912-3923.
Shimomura, K., Okura, T., Kato, S., Couraud, P. O., Scherrmann, J. M., Terasaki, T. and Deguchi, Y. (2013) Functional expression of a proton-coupled organic cation (H^+/OC) antiporter in human brain capillary endothelial cell line hCMEC/D3, a human blood-brain barrier model. *Fluids Barriers CNS* **10**, 8.

Suzuki, T., Ohmuro, A., Miyata, M., Furuishi, T., Hidaka, S., Kugawa, F., Fukami, T. and Tomono, K. (2010) Involvement of an influx transporter in the blood brain barrier transport of naloxone. *Biopharm. Drug Dispos.* **31**, 243-252.

Tamai, I., Nakanishi, T., Kobayashi, D., China, K., Kosugi, Y., Nezu, J., Sai, Y. and Tsuji, A. (2004) Involvement of OCTN1 (SLC22A4) in pH-dependent transport of organic cations. *Mol. Pharm.* **1**, 57-66.

Tega, Y., Akanuma, S., Kubo, Y. and Hosoya, K. (2015a) Involvement of the H^+/organic cation antiporter in nicotine transport in rat liver. *Drug Metab. Dispos*. **43**, 89-92.

Tega, Y., Akanuma, S., Kubo, Y., Terasaki, T. and Hosoya, K. (2013) Blood-to-brain influx transport of nicotine at the rat blood-brain barrier: involvement of a pyrilamine-sensitive organic cation transport process. *Neurochem. Int.* **62**, 173-181.

Tega, Y., Kubo, Y., Yuzurihara, C., Akanuma, S. and Hosoya, K. (2015b) Carrier-mediated transport of nicotineAcross the Innerblood-retinal barrier: Involvement of a novel organic cation transporter driven by an outward $H^{(+)}$ gradient. *J. Pharm. Sci.* **104**, 3069-3075.

Tun, T. and Kang, Y. S. (2017) Imperatorin is transported through blood-brain barrier by carrier mediated transporters. *Biomol. Ther. (Seoul)* **25**, 441-451.

Wu, D., Kang, Y. S., Bickel, U. and Pardridge, W. M. (1997) Blood-brain barrier permeability to morphine-6-glucuronide is markedly reduced compared with morphine. *Drug Metab. Dispos.* **25**, 768-771.

Xie, Y., Zhou, H., Wong, Y. F., Xu, H. X., Jiang, Z. H. and Liu, L. (2008) Study on the pharmacokinetics and metabolism of paeonol in rats treated with pure paeonol and an herbal preparation containing paeonol by using HPLC-DAD-MS method. *J. Pharm Biomed. Anal.* **46**, 748-756.

Xu, D., Zhou, C. and Xu, B. (2008) Protective effect of paeonol on beta-amyloid 25-35 induced toxicity in PC12 cells. *Neural Regen. Res.* **3**, 863-866.

Xu, S. P., Sun, G. P., Shen, Y. X., Wei, W., Peng, W. R. and Wang, H. (2007) Antiproliferation and apoptosis induction of paeonol in HepG2 cells. *World J. Gastroenterol.* **13**, 250-256.

Zhao, Y., Fu, B., Zhang, X., Zhao, T., Chen, L., Zhang, J. and Wang, X. (2014) Paeonol pretreatment attenuates cerebral ischemic injury via upregulating expression of pAkt, Nrf2, HO-1 and ameliorating BBB permeability in mice. *Brain Res. Bull.* **109**, 61-67.

Zhong, S. Z., Ge, Q. H., Qu, R., Li, Q. and Ma, S. P. (2009) Paeonol attenuates neurotoxicity and ameliorates cognitive impairment induced by d-galactose in ICR mice. *J. Neurol. Sci.* **277**, 58-64.

Zhou, A., Wu, H., Pan, J., Wang, X., Li, J., Wu, Z. and Hui, A. (2015) Synthesis and evaluation of paeonol derivatives as potential multifunctional agents for the treatment of Alzheimer's disease. *Molecules* **20**, 1304-1318.

Zhou, J., Zhou, L., Hou, D., Tang, J., Sun, J. and Bondy, S.C. (2011) Paeonol increases levels of cortical cytochrome oxidase and vascular actin and improves behavior in a rat model of Alzheimer's disease. *Brain Res.* **1388**, 141-147.